

## Colossal dielectric constants in single-crystalline and ceramic $\text{CaCu}_3\text{Ti}_4\text{O}_{12}$ investigated by broadband dielectric spectroscopy

Stephan Krohns, Peter Lunkenheimer, Stefan G. Ebbinghaus, Alois Loidl

### Angaben zur Veröffentlichung / Publication details:

Krohns, Stephan, Peter Lunkenheimer, Stefan G. Ebbinghaus, and Alois Loidl. 2008.  
"Colossal dielectric constants in single-crystalline and ceramic  $\text{CaCu}_3\text{Ti}_4\text{O}_{12}$  investigated by broadband dielectric spectroscopy." *Journal of Applied Physics* 103 (8): 084107.  
<https://doi.org/10.1063/1.2902374>.

### Nutzungsbedingungen / Terms of use:

licgercopyright

Dieses Dokument wird unter folgenden Bedingungen zur Verfügung gestellt: / This document is made available under these conditions:

#### Deutsches Urheberrecht

Weitere Informationen finden Sie unter: / For more information see:

<https://www.uni-augsburg.de/de/organisation/bibliothek/publizieren-zitieren-archivieren/publiz/>



# Colossal dielectric constants in single-crystalline and ceramic $\text{CaCu}_3\text{Ti}_4\text{O}_{12}$ investigated by broadband dielectric spectroscopy

Cite as: J. Appl. Phys. **103**, 084107 (2008); <https://doi.org/10.1063/1.2902374>

Submitted: 08 October 2007 • Accepted: 22 January 2008 • Published Online: 22 April 2008

S. Krohns, P. Lunkenheimer, S. G. Ebbinghaus, et al.



View Online



Export Citation

## ARTICLES YOU MAY BE INTERESTED IN

$\text{CaCu}_3\text{Ti}_4\text{O}_{12}$ : One-step internal barrier layer capacitor

Applied Physics Letters **80**, 2153 (2002); <https://doi.org/10.1063/1.1463211>

Broadband dielectric spectroscopy on single-crystalline and ceramic  $\text{CaCu}_3\text{Ti}_4\text{O}_{12}$

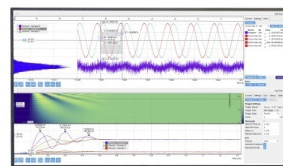
Applied Physics Letters **91**, 022910 (2007); <https://doi.org/10.1063/1.2757098>

Colossal dielectric constant up to gigahertz at room temperature

Applied Physics Letters **94**, 122903 (2009); <https://doi.org/10.1063/1.3105993>

Challenge us.

What are your needs for  
periodic signal detection?



Zurich  
Instruments



# Colossal dielectric constants in single-crystalline and ceramic $\text{CaCu}_3\text{Ti}_4\text{O}_{12}$ investigated by broadband dielectric spectroscopy

S. Krohns,<sup>1</sup> P. Lunkenheimer,<sup>1,a)</sup> S. G. Ebbinghaus,<sup>2</sup> and A. Loidl<sup>1</sup>

<sup>1</sup>*Experimental Physics V, Center for Electronic Correlations and Magnetism, University of Augsburg, 86135 Augsburg, Germany*

<sup>2</sup>*Solid State Chemistry, University of Augsburg, 86135 Augsburg, Germany*

(Received 8 October 2007; accepted 22 January 2008; published online 22 April 2008)

In the present work, the authors report results of broadband dielectric spectroscopy on various samples of  $\text{CaCu}_3\text{Ti}_4\text{O}_{12}$  (CCTO), also including single-crystalline material, which so far was only rarely investigated. The measurements extend up to 1.3 GHz, covering more than nine frequency decades. We address the question of the origin of the colossal dielectric constants and of the relaxational behavior in this material, including the second relaxation reported in several recent works. For this purpose, the dependence of the temperature- and frequency-dependent dielectric properties on different tempering and surface treatments of the samples and on ac-field amplitude is investigated. Broadband spectra of a single crystal are analyzed by an equivalent circuit description by assuming two highly resistive layers in series to the bulk. Good fits could be achieved, including the second relaxation, which also shows up in single crystals. The temperature- and frequency-dependent intrinsic conductivity of CCTO is consistent with the variable range hopping model. The second relaxation is sensitive to surface treatment and, in contrast to the main relaxation, is also strongly affected by the applied ac voltage. Concerning the origin of the two insulating layers, we discuss a completely surface-related mechanism by assuming the formation of a metal-insulator diode and a combination of surface and internal barriers.

© 2008 American Institute of Physics.

[DOI: [10.1063/1.2902374](https://doi.org/10.1063/1.2902374)]

## I. INTRODUCTION

For further technical advances in the performance and miniaturization of capacitive electronic elements, new materials with high dielectric constants ( $\epsilon'$ ) are urgently needed. Thus, since the first reports of extremely high (“colossal”) values of  $\epsilon'$  in  $\text{CaCu}_3\text{Ti}_4\text{O}_{12}$  (CCTO),<sup>1–3</sup> this material has been the focus of scientific research (see, e.g., Refs. 4–9) and more than 180 papers have been published on this topic in the past six years. In the early stages, various intrinsic mechanisms were proposed.<sup>2,3,10</sup> However, further investigations revealed strong hints that the colossal  $\epsilon'$  in CCTO is of nonintrinsic origin.<sup>4–7,9,11</sup> In a pioneering work, Sinclair *et al.*<sup>4</sup> plotted the results of their dielectric measurements on ceramic CCTO in the complex impedance plane representation, revealing a succession of two semicircles. Such a behavior is often found in ceramic materials, whose dielectric response at low frequencies is dominated by grain boundaries. Hence, these results were explained with an “internal barrier layer capacitor” (IBLC) model: Polarization is built up at insulating grain boundaries between the semiconducting grains of the ceramic samples. This generates nonintrinsic colossal values of the dielectric constant, which are accompanied by a strong Maxwell–Wagner (MW) relaxation mode. However, it should be noted that the impedance representation does not allow identification of the physical origin of the observed semicircles. The first semicircle could be due to grain boundaries, planar crystal defects (e.g., twinning

boundaries), insulating surface layers, or even an intrinsic relaxation. Indeed, based on measurements of ceramic CCTO samples, significant contributions from external surface effects were proposed by our group,<sup>9</sup> as we also detected in various other materials.<sup>8,12,13</sup> We found that sputtered contacts give rise to a  $\epsilon'$  much higher than that of silver-paint contacts and that  $\epsilon'$  depends on sample thickness. Very recently, we reported a similar behavior for single-crystalline samples, too.<sup>14</sup> These results can be explained within a “surface barrier layer capacitor” (SBLC) picture by assuming, e.g., the formation of a Schottky diode at the contact-bulk interface.<sup>9</sup>

Nevertheless, it is frequently stated in current literature that the IBLC is the more likely mechanism. To a large extent, this notion is based on results for ceramic samples with different grain sizes, which are prepared, e.g., by subjecting the samples to various heat treatments. This was shown to result in a strong variation in the absolute values of  $\epsilon'$  and conductivity  $\sigma'$ , thus supporting the SBLC picture (e.g., Refs. 11, 15, and 16). However, it should be noted that extremely high values of  $\epsilon'$  were particularly observed in CCTO single crystals (SCs),<sup>3</sup> in which grain boundaries are absent. Thus, other internal boundaries in SCs, e.g., twin boundaries, were considered.<sup>4,6,17</sup> However, if there are any planar defects in SCs that generate high dielectric constants and strong relaxations, they may be expected to also contribute to a separate relaxational response in polycrystals (PCs), in which the grains are often rather large (up to 100  $\mu\text{m}$ ). In this case, in PCs, two relaxations should be observed, one

<sup>a)</sup>Electronic mail: peter.lunkenheimer@physik.uni-augsburg.de.

TABLE I. Sample parameters. The grain sizes are rough estimates only, which were obtained from ESEM measurements.

Sample	Figure	Area (mm <sup>2</sup> )	Thickness (mm)	Grain size (μm)
SC	1–4	16.6	1.10	Not applicable
PC 1, 3 h tempered	5	24.0	1.24	2–6
PC 2, 48 h tempered	5	32.6	1.20	80–200
PC 3, 48 h tempered, before polishing	6(a) and 6(d)	22.9	1.63	80–200
PC 3, 48 h tempered, after polishing	6(b), 6(e), 6(c), and 6(f)	22.9	1.55	80–200

from planar defects and the other one originating from the grain boundaries. Interestingly, there is indeed evidence for at least two relaxations in CCTO. In one of the earliest reports on CCTO,<sup>2</sup> indications of a second relaxation were already obtained and since then various experiments revealed that it is quite a common feature of PC CCTO.<sup>9,10,14,15,18,19</sup> This relaxation results in  $\epsilon'$  values that are even larger than those of the famous main relaxation, although at lower frequencies and/or higher temperatures only. However, in contrast to the above-mentioned scenario, wherein the two relaxations should arise from grain boundaries and planar defects within the grains, an alternative explanation is also possible. Namely, one relaxation could be due to an IBLC and the other to a SBLC mechanism,<sup>9,14</sup> a notion that would provide a solution to the SBLC/IBLC debate.

Obviously, there are many open questions concerning the origin of the dielectric properties of CCTO. In the present work, we contribute to their solution by providing dielectric results on various samples that were subjected to different tempering and surface treatments. The dielectric constant, loss, and conductivity were determined in a broad frequency range of nine frequency decades, up to 1.3 GHz, which is of major relevance for possible high-frequency applications. The measurements also include single-crystalline samples, which so far were only rarely studied.<sup>3</sup> The present work extends our previous study on single- and polycrystalline CCTO wherein we reported evidence for a second relaxation also in SCs and a strong influence of surface treatments on the dielectric properties.<sup>14</sup> Here, we provide additional experimental data and a more detailed analysis. Among others, we have performed fits of the obtained spectra by using an equivalent circuit approach and show data for samples subjected to different tempering treatments. In addition, the ac voltage dependence of dielectric constant and conductivity spectra is also shown.

## II. EXPERIMENTAL DETAILS

Polycrystalline samples of CCTO were prepared as reported in Ref. 9 and sintered at 1000 °C in air for up to 48 h. SCs were grown by the floating zone technique.<sup>3,14</sup> The applied growth furnace (model GERO SPO) is equipped with two 1000 W halogen lamps, the radiation of which is focused by gold-coated ellipsoidal mirrors. PC bars serving as seed and feed rods were cold pressed and sintered in air for 12 h at 1000 °C. The seed rod was rotated with a speed of 30 rpm, while the feed was kept still. To avoid thermal reduction of copper, crystal growth was performed in oxygen

(flow rate of 0.2 l/min) at a pressure of 4 bar and a growth rate of 5 mm/h was applied. Although this rate is rather fast for the traveling solvent floating zone method, it could be used since the composition of the eutectic is close to the desired stoichiometry, i.e., the CCTO pseudocongruently melts. From the obtained crystal boules, thin disks were cut and polished. The quality of the crystal was checked by Laue backscattering diffraction. All diffraction patterns obtained from different spots of both sides of the disk could be fully indexed by using the space group and cell parameters of CCTO and the same orientation matrix. Thus, no hints for a twinning were found although the possibility of merohedral twinning cannot be excluded. The surface topographies of the samples were investigated by using an environmental scanning electron microscope (ESEM) (ESEM XL30, FEI Company) with an accelerating voltage of 15 kV. Operating in a low-hydrogen-pressure atmosphere prevents charging effects without contacting the sample surface.

For the dielectric measurements, silver-paint or sputtered gold contacts (thickness of 100 nm) were applied to opposite sides of the platelike samples after cleaning the surfaces with isopropanol. Some samples were subjected to different sintering and surface treatments, as will be described in Sec. III. All sintering procedures were performed on samples, which had no contacts, to avoid diffusion effects of the contact material. For some PCs, a possible surface layer of different stoichiometry was removed by polishing with superfine sandpaper (grit size of P1200). The complex conductivity  $\sigma^* = \sigma' + i\sigma''$  and permittivity  $\epsilon^* = \epsilon' - i\epsilon''$  were measured over a frequency range of up to nine decades (1 Hz <  $\nu$  < 1.3 GHz) at temperatures down to 40 K, as detailed in Refs. 9 and 20. In most experiments, the applied ac voltage was 1 V. In addition, measurements up to 15 V were also performed. The geometry and typical grain sizes of the samples, for which results are shown in the present work, are given in Table I. The experimental results for samples treated in the same way (the same thermal history, the same contact preparation, and the same surface treatment) were highly reproducible.

## III. RESULTS AND DISCUSSION

### A. Temperature dependence

Figures 1(a) and 1(b) show the temperature dependences of the dielectric constant and conductivity of single-crystalline CCTO for various frequencies. This representation corresponds to that used in Fig. 2(a) of the pioneering work of Homes *et al.*<sup>3</sup> Here, we provide data on one SC,

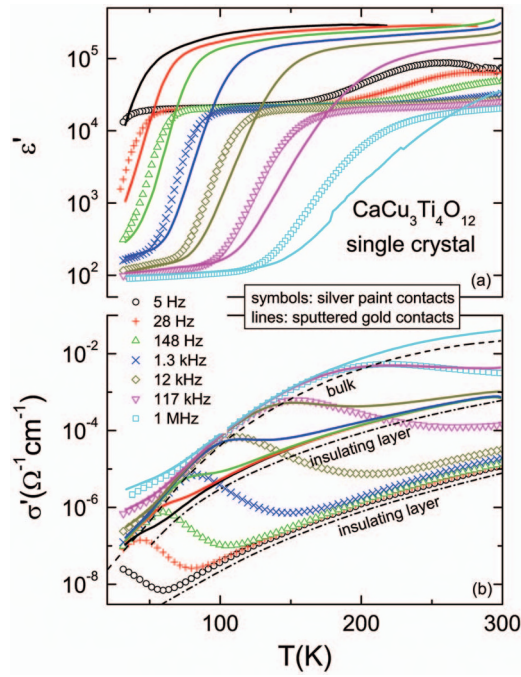


FIG. 1. (Color) Temperature-dependent dielectric constants (a) and conductivities (b) of single-crystalline CCTO with sputtered gold (solid lines) and silver-paint contacts (symbols) at various frequencies (lines and symbols of the same frequency have the same color). The dashed and dashed-dotted lines in (b) give an estimate of the intrinsic bulk dc conductivity (the same for both measurements) and the contribution of the insulating layer (different), respectively. For clarity reasons, these lines were slightly shifted downward.

which was measured with two different types of contacts (silver-paint and sputtered gold). In both cases, at low frequencies and high temperatures, colossal values of the dielectric constant show up. With  $\epsilon'_{\text{high}} \approx 2 \times 10^5$ , they are significantly higher for the sputtered than for the silver-paint contacts. This agrees with our findings from frequency-dependent data on PCs (Ref. 9) and SCs,<sup>14</sup> which were interpreted by assuming a surface-related origin of the high  $\epsilon'$  values.<sup>9</sup> The well-known relaxation mode of CCTO shows up as a steplike decrease in  $\epsilon'$  with decreasing temperature, which shifts to higher temperatures with increasing frequency. It is now generally accepted that this relaxation is of MW type, and caused by an equivalent circuit consisting of the bulk contribution, which is connected in series to a parallel RC circuit where  $R$  and  $C$  are much higher than the corresponding bulk quantities. The highly resistive thin layers that generate this RC circuit could be surface layers, grain boundaries, or planar defects.

Interestingly, in the  $\epsilon'(T)$  results obtained with silver-paint contacts, a second relaxation mode is detected. It leads to an increase in the dielectric constant, e.g., at  $T > 180$  K for 5 Hz, which is superimposed onto the high  $\epsilon'$  plateau of the main relaxation mode. This finding is consistent with the detection of a second relaxation in the dielectric spectra of single-crystalline CCTO that we reported in Ref. 14 [see also Fig. 3(a)]. The occurrence of a second relaxation also in SCs excludes one of the scenarios mentioned in Sec. I: As the effect of grain boundaries in SCs is expected to be negli-

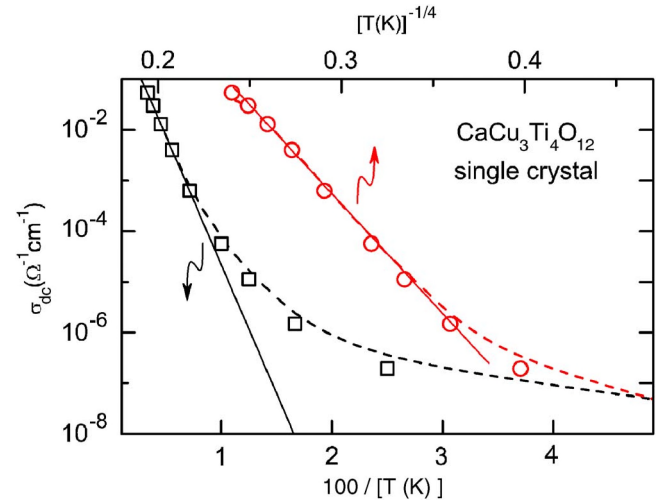


FIG. 2. (Color online) Dashed lines: Temperature dependence of the dc conductivity approximated by the dashed line shown in Fig. 1(b). In addition, results for  $\sigma_{\text{dc}}$  from the fits of the frequency dependence (Fig. 3) are shown (symbols). Both data sets are provided in two representations that should lead to a linearization for the Arrhenius and VRH behavior indicated by the solid lines.

gible, it is not possible to explain the two relaxations in CCTO by separate contributions from grain boundaries and planar defects.

The conductivity, shown in Fig. 1(b), is directly related to the dielectric loss  $\epsilon''$  via  $\sigma' = 2\pi\nu\epsilon''\epsilon_0$  ( $\epsilon_0$  is the permittivity of free space). Thus, its temperature dependence is identical to that of the loss and it exhibits the well-known peaks and their characteristic shift with frequency. However, in contrast to the loss representation,<sup>3</sup> in the conductivity representation, the peaks merge at low temperatures for  $\nu > 100$  Hz. This is the case not only for different frequencies of a single sample preparation but also for the measurements with different contact types shown in Fig. 1(b). This behavior is due to the fact that at the low-temperature wing of these peaks, the condition  $\nu > 1/(2\pi\tau)$  is fulfilled, where  $\tau$  is the relaxation time of the equivalent circuit. Thus, here, the capacitances of the insulating layers are shorted and the intrinsic dc conductivity of CCTO is detected. Its temperature dependence is indicated by the uppermost dashed line in Fig. 1(b) (for better readability, it is slightly shifted downward). The deviations from this line that show up, e.g., below about 70 K for 1 MHz point to a frequency dependence of the intrinsic  $\sigma'$  due to hopping charge transport.<sup>21</sup>

In Fig. 2, we show the bulk dc conductivity, which is approximated by the dashed line in Fig. 1(b), in an Arrhenius representation (dashed line, lower scale). In addition,  $\sigma_{\text{dc}}$  results from the fits of frequency-dependent data discussed below are included as squares. As indicated by the solid line, only in a rather restricted range at high temperatures do the data follow the thermally activated Arrhenius behavior.<sup>22</sup> As an alternative, the same data are also shown in a representation that leads to linear behavior for three dimensional variable range hopping (VRH) (upper scale).<sup>23</sup> Indeed, in a large temperature region, the data follow the prediction of this model. The VRH behavior in CCTO was also reported in Ref. 24 but it was based on data within a smaller temperature



range only. Within this model, a frequency dependence of the conductivity,  $\sigma' = \sigma_{dc} + \sigma_0 \omega^s (s < 1)$ , is predicted. This explains the mentioned intrinsic frequency dependence of  $\sigma'$  below roughly 70 K [Fig. 1(b)].

At high temperatures, the  $\sigma'(T)$  curves also merge but approach two different curves for the two contact types (dashed-dotted lines). Here, the conductivity is dominated by the highly resistive layer and, obviously, its resistance differed by about two decades for the two types of contact preparations. In Ref. 9, the very different values of  $\epsilon'_{\text{high}}$  that were obtained for sputtered and silver-paint contacts were interpreted by assuming a surface-related origin of the high  $\epsilon'$  values via the formation of Schottky diodes at the contact-bulk interface. It was assumed that a different surface wetting of these contact types, arising from larger air gaps at the interface for silver-paint contacts,<sup>8,25</sup> should lead to a less effective formation of the Schottky diodes.<sup>8</sup> One can speculate that this may also explain the very different high-temperature behavior of the conductivity observed in Fig. 1(b). An alternative explanation for the marked differences in the dielectric properties of CCTO measured with different contact materials could be that due to their grain structure and the air gaps, silver-paint contacts are generally unsuited for the measurements of very high dielectric constant materials. However, we demonstrated in two earlier works<sup>9,26</sup> that for intrinsic  $\epsilon'$  values of up to  $2 \times 10^4$  and  $2 \times 10^5$ , silver-paint contacts lead to the same results as sputtered gold. Even the intrinsic values of  $\epsilon'$  exceeding  $10^7$  that were observed in o-TaS<sub>3</sub>, a typical charge density wave system,<sup>27</sup> could be properly measured by using silver-paint contacts.<sup>28</sup>

## B. Frequency dependence

Figure 3 shows the broadband spectra of dielectric constant, loss, and conductivity for single-crystalline CCTO with contacts formed by silver paint. The most obvious differences with the corresponding figure for sputtered contacts<sup>14</sup> are the lower values of the dielectric constant  $\epsilon'_{\text{high}}$  (cf. inset) and the clear occurrence of a second relaxation at low frequencies. Both features are also revealed in the temperature-dependent data (Fig. 1). The MW relaxation modes show up as steplike decreases in  $\epsilon'(\nu)$ , shifting through the frequency window with temperature. Correspondingly, peaks in the loss  $\epsilon''(\nu)$  and shoulders in  $\sigma'(\nu)$  are revealed. Considering the above-mentioned equivalent circuit, at high frequencies, the highly resistive thin layers (surface layers, grain boundaries, or planar defects) that generate the  $RC$  circuit in series to the bulk are shorted via their capacitance and the intrinsic behavior is detected. This is nicely demonstrated in Fig. 4, in which the frequency-dependent dielectric constant and conductivity for the two contact types are compared. While at low frequencies strong differences show up, the intrinsic properties of CCTO governing the high-frequency behavior remain unaffected by the contact variation. They reveal a rather high dielectric constant of about 85 and a succession of dc and ac conductivities, which is characteristic of hopping of localized charge carriers.<sup>9,29</sup> The latter is consistent with our finding of VRH from the dc conductivity (Fig. 2).<sup>21,23</sup>

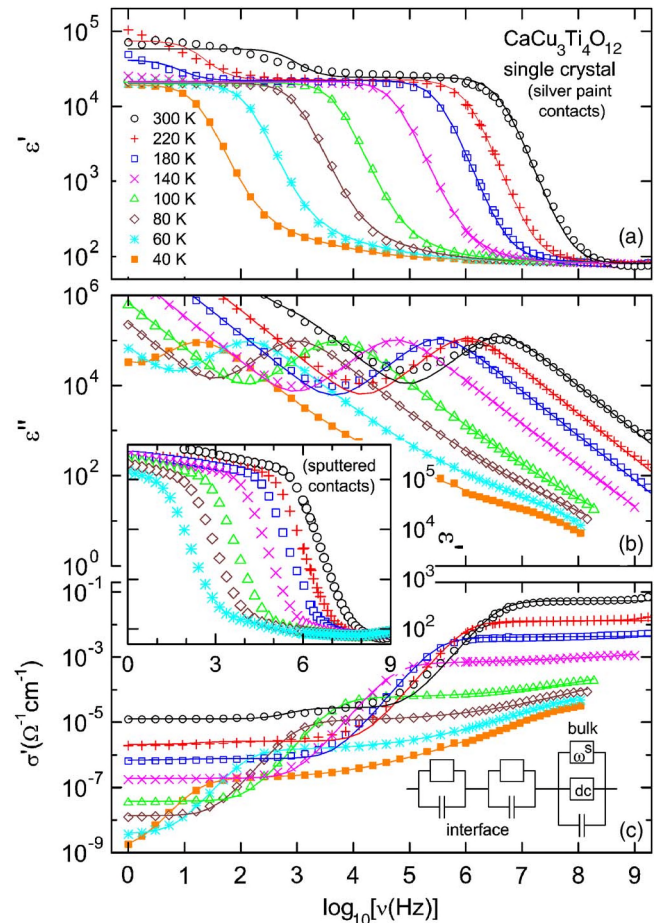


FIG. 3. (Color online) Frequency-dependent dielectric constants (a), losses (b), and conductivities (c) of single-crystalline CCTO with silver-paint contacts at various temperatures. The data are fitted with the equivalent circuit indicated in (c) (Ref. 9). The inset shows  $\epsilon'$  for the same sample using sputtered gold contacts (Ref. 14).

To account for the second relaxation, an additional  $RC$  element in the equivalent circuit has to be assumed. By adding a further element for the mentioned frequency-dependent conductivity, we arrive at the circuit shown in Fig. 3(c), which was also used in Ref. 9 for the analysis of the behavior of PCs. The lines in Fig. 3 are least-square fits with this model, leading to a reasonable agreement between experimental data and fits. Only the second relaxation in  $\epsilon'(\nu)$  is not perfectly covered: The experimental relaxation steps are more smeared out than the fit curves. This points to a distribution of relaxation times of the circuit due to heterogeneities. Depending on the interpretation of this relaxation, they may be generated, e.g., by surface roughness or a distribution of grain sizes. In Figs. 1 and 3, while the relaxation steps in  $\epsilon'$  are also accompanied by corresponding features in  $\epsilon''$  and  $\sigma'$  (a peak and a shoulder, respectively), this does not seem to be the case for the second relaxation. However, taking a closer look at Fig. 3(c), a small shoulder, e.g., at about  $10^3$  Hz for 300 K, is observed. This becomes especially obvious in the fits, which slightly exaggerate this feature. If we ascribe the two  $RC$  circuits to two different types of insulating layers, the sum of their resistances dominates the conductivity at the lowest frequencies. For the 300 K curve in Fig. 3(c), for  $\nu > 10^3$  Hz, one circuit becomes shorted, which

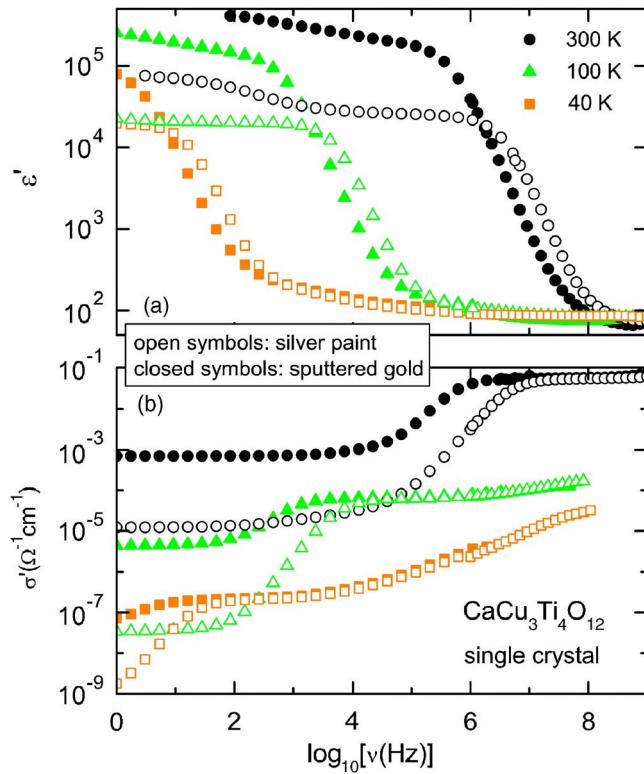


FIG. 4. (Color online) Frequency-dependent dielectric constants (a) and conductivities (b) of single-crystalline CCTO with silver-paint contacts (open symbols) and sputtered gold (closed symbols) at selected temperatures.

leads to the small shoulder and the corresponding relaxation step in  $\varepsilon'$  [Fig. 3(a)]. Obviously, the resistances of both layers are of similar magnitude, which explains the small effect in  $\sigma'$  and the directly related  $\varepsilon''$ . This is corroborated by the results from the equivalent circuit analysis: With values of 14.4 and 4.2 nF at 300 K, the capacitances of the two layers differ more than the resistances do (37.6 and 14.6 k $\Omega$ , respectively). As expected, the bulk capacitance (10.7 pF) and resistance (12.2  $\Omega$ ) are much smaller than those of the layers. The temperature-dependent conductivity values that were calculated from the obtained bulk resistances for different temperatures are shown in Fig. 2. They agree well with the intrinsic dc conductivity that was estimated from the temperature-dependent plot of Fig. 1(b).

It is well known that the dielectric properties of CCTO PCs are qualitatively similar to those of SCs but they usually reveal a lower range of the dielectric constant  $\varepsilon'_{\text{high}}$ . However, as recently shown, when using sputtered contacts and subjecting the samples to long sintering procedures, values up to  $10^5$  can be also reached in PCs.<sup>14</sup> To systematically study the effect of different tempering times, we used silver-paint contacts, which, in contrast to sputtered contacts, can be easily removed by dissolving. Figure 5 shows two typical results of our sintering experiments:  $\varepsilon'_{\text{high}}$  strongly increases when tempering the sample for 48 h. A sample tempered for 24 h (not shown) revealed  $\varepsilon'_{\text{high}}$  values between those of the 3 and 48 h tempered samples. At the limit of high frequencies and low temperatures, similar intrinsic  $\varepsilon'$  and  $\sigma'$  values are reached, as expected for MW relaxations. Within the IBLC

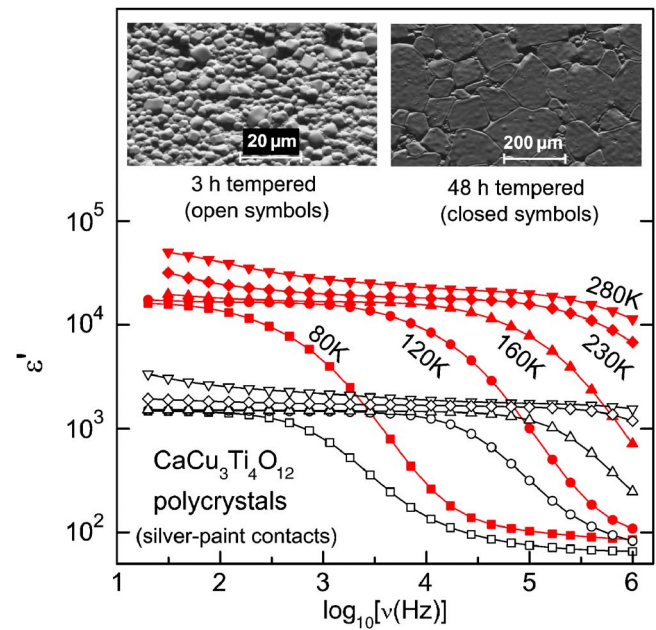


FIG. 5. (Color online) Frequency-dependent dielectric constants of ceramic CCTO samples tempered for 3 h (open symbols) and 48 h (closed symbols) with silver-paint contacts. The insets show the surface topographies obtained by ESEM.

framework, the strong tempering effect on  $\varepsilon'_{\text{high}}$  can be ascribed to the growth of grain sizes.<sup>11,15,16</sup> However, as an alternative, it can be also explained in terms of the different surface topographies revealed by ESEM (insets of Fig. 5). When the grains are growing during sintering, the surface of the samples obviously becomes much smoother. Thus, the effect of tempering could be quite the same as that of using sputtered contacts instead of silver paint: Just in the same way that the smaller particles of sputtered contacts lead to an increase in the direct contact area between the rough sample surface and the metallic contact material,<sup>8,9</sup> the smoother sample surface could also result in a better “wetting” of the contact.<sup>25</sup> If one assumes that the formation of a Schottky diode leads to an insulating depletion layer at the contact to the semiconducting CCTO sample, this better wetting should cause an increase in  $\varepsilon'_{\text{high}}$ , as is indeed observed in Fig. 5. Overall, as the tempering obviously also has an effect on the sample surface, it is difficult to draw definite conclusions from such experiments.

### C. Second relaxation

In all the figures shown so far, at low frequencies and/or high temperatures, there are at least indications of the mentioned second relaxation. As for the main relaxation, for the second relaxation, three possible origins have to be also considered: intrinsic, IBLC, or a surface layer. An intrinsic mechanism is highly unlikely because the magnitude of this relaxation considerably varies for different samples (see present work and Refs. 2, 9, 10, 14, 15, 18, and 30). In Ref. 30, an intrinsic relaxor ferroelectric behavior was proposed based on the occurrence of broad dielectric peaks in  $\varepsilon'(T)$  at low frequencies and high temperatures. In fact, in the present work, such temperature dependence is observed, too: It is revealed by the peaklike behavior of  $\varepsilon'(T)$  at 5 Hz in Fig.

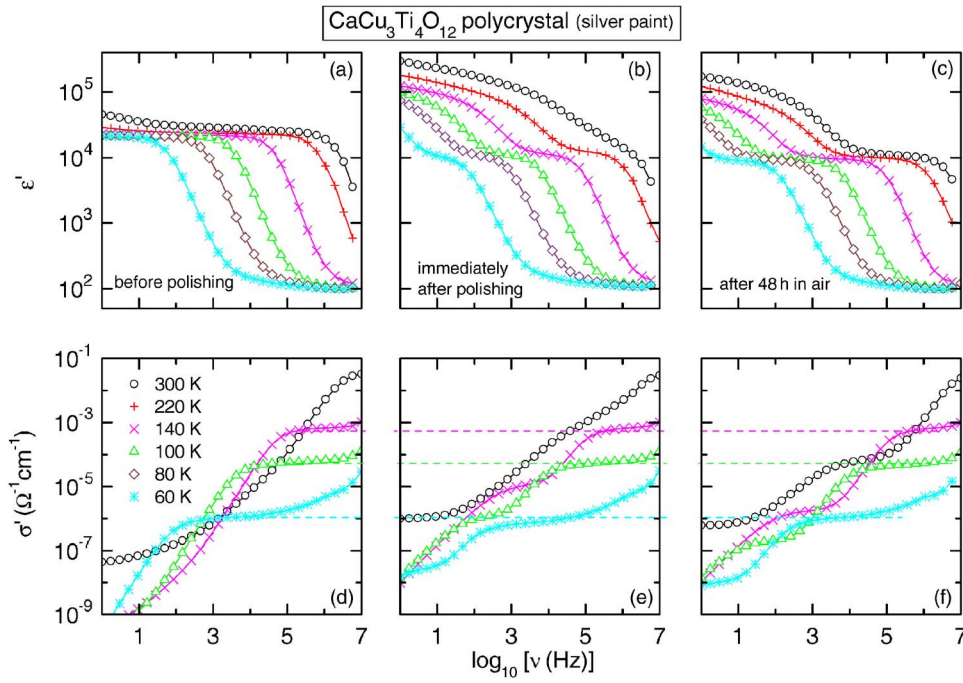


FIG. 6. (Color online) Frequency-dependent dielectric constants [(a)–(c)] and conductivities [(d)–(f)] of polycrystalline CCTO (tempered for 48 h) with silver-paint contacts at various temperatures. Results are shown for the untreated sample [(a) and (d)], after polishing under  $N_2$  atmosphere [(b) and (e)] with both contacts reapplied, and after leaving it in air (without silver-paint contacts) for 48 h [(c) and (f)].

1(a) as well as by the crossing of the curves for 220 and 300 K at low frequencies in Fig. 3(a). However, such behavior can also arise within an equivalent circuit description with temperature-independent capacitors (to keep it simple, in the following, we assume only a single  $RC$  circuit in series to the bulk). For example, by making the reasonable assumption that the insulating-layer capacitance  $C_i$  is much larger than the bulk capacitance  $C_b$ , the overall capacitance in the limit of small frequencies is given by  $C_0 = C_i G_b^2 / (G_b + G_i)^2$  ( $G_b$  and  $G_i$  denote the bulk and insulating-layer conductances, respectively). For  $G_b \gg G_i$ ,  $C_0 \approx C_i$  is obtained, but if  $G_b(T)$  and  $G_i(T)$  should become of similar magnitude at high temperatures,  $C_0$  can decrease to  $C_i/4$ . Together with the decrease in  $\varepsilon'$  with decreasing temperature due to the MW relaxation, this can lead to a peak. Thus, the temperature dependence of  $G_b$  and  $G_i$  can result in a maximum in  $C_0$  and, thus, also in the low-frequency  $\varepsilon'(T)$ , as observed in Ref. 30 and Fig. 1(a).

In our search for the origin of the second relaxation, we found a strong effect when removing the surface layers of a PC by polishing.<sup>31</sup> The polishing reduced the original sample thickness of 1.63 mm by about 0.08 mm (Table I). Judging from our thickness-dependent experiments in Ref. 9, the mere thickness variation should lead to a change of  $\varepsilon'$  not exceeding 5%. To take into account the possible presence of a surface layer with different stoichiometry, the polishing was done under a  $N_2$  atmosphere to avoid any reaction with oxygen at the freshly exposed surface. Afterward, the sample was installed in the vacuum of the cryostat as fast as possible. Figure 6 shows the results for the untreated sample [Figs. 6(a) and 6(d)], immediately after polishing [Figs. 6(b) and 6(e)], and after leaving it in air for 48 h [Figs. 6(c) and 6(f)]. In the dielectric constant of the untreated sample [Fig. 6(a)], the second relaxation is only weakly seen at best. After polishing, it becomes very prominent [Fig. 6(b)]. It again seems to weaken when exposed to air (with removed silver-

paint contacts) and a shift of the relaxation steps to lower frequencies is observed [Fig. 6(c)]. The conductivities plotted in Figs. 6(d)–6(f) also show some significant and interesting effects: The intrinsic properties remain unaffected; e.g., the bulk dc conductivity, which is indicated by the horizontal dashed lines, is identical for all three cases. However, the downward step in  $\sigma'(\nu)$ , which precedes the dc plateau, reveals strong differences: Its lower plateau value, which is seen at room temperature at the lowest frequencies only, is much smaller for the untreated sample. For the treated samples, an intermediate plateau shows up (e.g., for 140 K at  $\sigma' \approx 10^{-5} \Omega^{-1} \text{ cm}^{-1}$  and  $\nu \approx 10^3 \text{ Hz}$ ). After 48 h of exposure to air, it becomes significantly reduced. Considering the equivalent circuit shown in Fig. 1(c), the first plateau at the lowest frequencies (seen at room temperature only) is determined by the resistance of the first  $RC$  circuit, the intermediate plateau by that of the second circuit, and the third one by the bulk conductivity.

The results in Fig. 6 seem to indicate that the second relaxation is influenced by surface effects and exchange with atmosphere. Thus, based on the experimental results of the present and earlier works of our group,<sup>8,9,14</sup> it is suggestive to assume a surface-generated origin of both relaxations in CCTO. Then, the second relaxation should be caused by a second surface layer. A possible explanation of such a layer arises from the fact that CCTO, like other transition metal oxides, strongly tends to the development of oxygen understoichiometry during preparation.<sup>4</sup> This leads to the introduction of charge carriers and an increase in  $\sigma'$ . However, one may speculate that at the surface of the samples, an exchange with ambient atmosphere leads to a layer, which is closer to the ideal stoichiometry and, thus, more insulating than the bulk.<sup>19</sup> However, there are also other possibilities: For example, chemical decomposition into more simple oxides could occur at the surface, also leading to a thin insulating layer. Within these scenarios, the polishing either has only



partly removed the surface layer, reducing its thickness and, thus, increasing the apparent static  $\varepsilon'$  of the second relaxation, or it was completely removed. In the latter case, the high  $\varepsilon'$  should be due to the development of a very thin new layer during the time when the sample was exposed to air during insertion into the cryostat. However, it is not clear if this could happen during this rather short time of about 3 min. Another explanation is that in a  $N_2$  atmosphere, decomposition can occur at the surface of the sample.<sup>19</sup> In any case, the fact that the relaxation varies with time when the sample is left in air [Figs. 6(c) and 6(f)] demonstrates that the second relaxation is sensitive to exchange with the surrounding atmosphere. This excludes other scenarios, e.g., a possible deterioration of the crystal structure at the surface by polishing, as it is known from Si wafers. In the picture of a surface layer generated by a different oxygen stoichiometry, the effect of air exposure leads to the growth of the thickness of the insulating layer; thus, the capacitance decreases, as observed at low frequencies in Figs. 6(b) and 6(c).

If indeed there is an insulating layer of a different stoichiometry at the surface of the samples, earlier arguments invoking the formation of Schottky diodes at the contact-bulk interfaces are no longer valid. Instead, we would have the situation of a metal covering a thin insulating layer on top of a semiconductor. This should lead to the generation of a so-called metal-insulator-semiconductor (MIS) diode, which is well known from electronic textbooks, forming a part of field effect transistors. In this scenario, a depletion layer forms just as in the case of a conventional diode but it is situated at the surface of the bulk semiconductor, which is just below the insulating layer.<sup>32</sup> Interestingly, a very recent investigation of the  $I$ - $V$  and  $C$ - $V$  characteristics has indeed revealed evidence for the MIS diode formation at the surface of thin CCTO films.<sup>33</sup> As for a conventional diode a strong effect of different wetting can also be expected for MIS diodes. This model implies the following succession of layers (starting from the inside): semiconducting bulk/depletion layer with lower conductance/insulating chemically different layer with lowest conductance/metal. In  $\sigma'(\nu)$ , with increasing frequency, one should thus see a transition from the very low conductivity arising from the insulating nonstoichiometric layer to the higher conductivity related to the depletion layer, which is followed by another steplike increase towards the intrinsic bulk conductivity. Such a behavior is indeed revealed in Figs. 6(e) and 6(f). However, within this framework, it is not straightforward to explain the variation of the absolute values of the conductivity, especially those of the above-mentioned intermediate plateau. It is likely that the variation of this plateau value, via the relaxation time of the equivalent circuit, leads to the strong frequency shift of the second relaxation when the sample is subjected to air for 48 h [compare Figs. 6(b) and 6(c)]. One could even speculate that for the untreated sample, the intermediate plateau is several decades lower (on the order of  $10^{-7}$  for room temperature) and, thus, the second relaxation is located below the lowest measuring frequency and of similar magnitude as for the treated samples. Thus, it is not clear if indeed the thick-

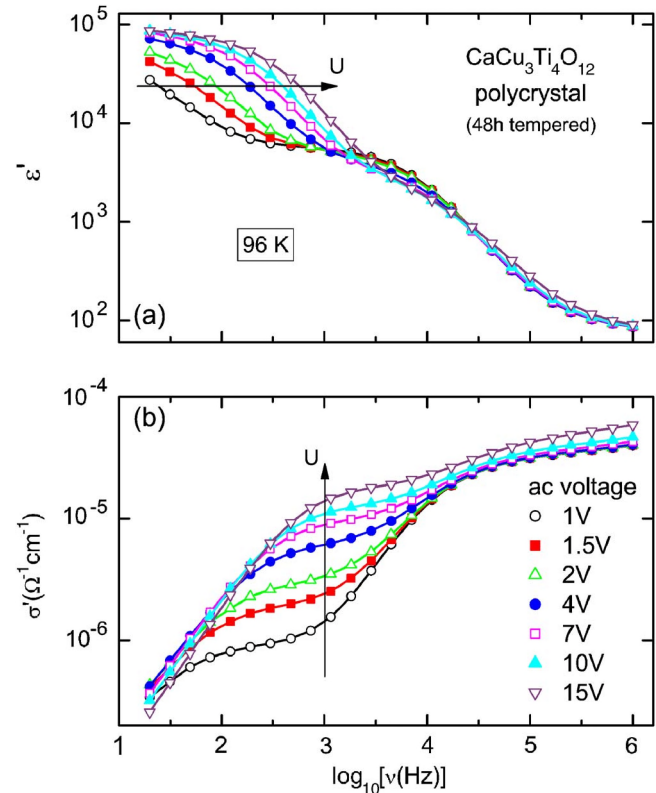


FIG. 7. (Color online)  $\varepsilon''(\nu)$  (a) and  $\sigma'(\nu)$  (b) at 96 K for different ac voltages. The same ceramic sample as in Figs. 6(c) and 6(f) was investigated.

ness of the different-stoichiometry surface layer or the conductance of the depletion layer, i.e., the effectiveness of the depletion, changes in Fig. 6.

## D. Voltage dependence

If any kind of diode formation plays a role in the generation of the dielectric behavior of CCTO, a nontrivial dependence of the dielectric behavior on the ac voltage should result. Thus, the dielectric spectra of the 48 h tempered polished PC, wherein both relaxations are well developed [cf. Fig. 6(c)], were measured for different voltages at 96 K. The results, which are shown in Fig. 7, reveal a strong dependence of the frequency of the second relaxation step on the ac voltage, while the main relaxation practically remains unaffected. Also, the intermediate plateau value of  $\sigma'(\nu)$  is strongly voltage dependent. To explain these findings, let us consider the equivalent circuit shown in Fig. 1. We make the assumption that  $C_b \ll C_1 \ll C_2$  and  $R_b \ll R_1 \ll R_2$  (the indices 1 and 2 denote the elements of the two  $RC$  circuits and  $b$  denotes the intrinsic bulk behavior). Then, the relaxation time of the main relaxation is approximately given by  $\tau_{\text{main}} \approx R_b C_1$ . The capacitance  $C_1$  corresponds to the plateau value  $\varepsilon'_{\text{high}}$  of the main relaxation [e.g.,  $\varepsilon'_{\text{high}} \approx 5 \times 10^3$  in Fig. 7(a)]. Obviously, it is not or only weakly dependent on voltage. It is also plausible that the bulk conductivity, which can be read off above about  $3 \times 10^4$  Hz in Fig. 7(b), is independent of voltage. This explains the absence of any significant variation of the main relaxation step in Fig. 7(a). The relaxation time of the second, low-frequency relaxation can be approxi-

mated by  $\tau_{\text{second}} \approx R_1 C_2$ . Judging from Fig. 7(a),  $C_2$  leading to the low-frequency plateau of  $\epsilon'(\nu)$  (about  $10^5$ ) seems to be constant. However,  $R_1$ , leading to the intermediate plateau in  $\sigma'(\nu)$  between  $10^2$  and  $10^4$  Hz in Fig. 7(b), is strongly voltage dependent. This explains the voltage-dependent shift of the second relaxation observed in Fig. 7(a).

The voltage dependence of  $R_1$  may well reflect the nonlinear  $I$ - $V$  characteristics of a diode. This is consistent with the MIS diode framework mentioned above. Within this picture,  $C_2$  corresponds to the capacitance of the insulating surface layer, which can be expected to be insensitive to voltage, as is indeed observed. However, in contrast to this completely SBLC dominated picture, the results of Fig. 7 can also be explained by assuming a combination of a SBLC and an IBLC mechanism: It is clear that the second relaxation is generated by the second  $RC$  circuit composed of  $R_2$  and  $C_2$ . However, the variation in its relaxation time that leads to the observed shift in Fig. 7(a) is completely due to the variation of the first  $RC$  circuit, namely, of  $R_1$ . Thus, Fig. 7 does only imply that the first relaxation caused by  $R_1$  and  $C_1$  arises from a diode (the origin of which is still to be clarified), but this cannot be said for the second relaxation. Instead, the latter could be due to the planar defects mentioned in Sec. I. Then, we could have Schottky diodes at the metal-bulk interface causing the first relaxation and planar defects (not grain boundaries) causing the second relaxation. Even the results in Fig. 6 may be explained in this way: As mentioned above, the strong differences between the appearances of the second relaxation that were caused by applying different surface treatments could be predominantly ascribed to a variation in its relaxation time. In this way, the observed surface sensitivity of the second relaxation could be due to the variation in  $R_1$  of the first  $RC$  circuit, i.e., the contact resistance. Within this model, it is this resistance that corresponds to the above-mentioned strongly varying intermediate plateau in Figs. 6(d)–6(f). However, it is not clear why the polishing and air exposure should lead to such a strong variation, while the capacitance  $C_1$  is only weakly affected [see plateau values of  $\epsilon'_{\text{high}} \approx 10^4$  in Figs. 6(a)–6(c)]. In addition, a close inspection of Fig. 6 seems to also reveal an amplitude variation of the second relaxation, which cannot be explained in this way.

#### IV. SUMMARY AND CONCLUSIONS

In summary, we performed detailed dielectric measurements on various CCTO samples subjected to different surface and heat treatments. Our study includes single-crystalline samples, which so far were only rarely investigated and covers a frequency range of up to 1.3 GHz. We found a strong variation in  $\epsilon'$  with contact material also in SCs of CCTO. Besides the well-known main relaxation, indications for a second relaxation are found in most of our measurements, including SCs. This leads to the conclusion that there must be two different types of insulating layers in CCTO. Indeed, by using an equivalent circuit that takes this notion into account, reasonable fits of the spectra extending over nine frequency decades could be achieved. Its origin so far is unclarified and it is also not clear if its varying visibil-

ity in different samples is due to a variation in its amplitude or relaxation time. As we also detected the second relaxation in SCs, grain boundaries may not play any role. However, of course, there is no such thing as a perfect SC and some “intrinsic” IBLC mechanism, such as twinning boundaries or microscopic electronic phase separation,<sup>34</sup> cannot be excluded. Interestingly, we found that the relaxation time and amplitude of the second relaxation sensitively depend on surface treatment<sup>14</sup> and ac voltage.

There are two alternative explanations for our experimental findings. For the first one, we consider the presence of a thin surface layer with different stoichiometry, leading to the formation of a MIS diode at the sample surface. Within such a completely surface-dominated picture, we can explain most of our own results, but clearly, this is at variance with the numerous reports evidencing an IBLC mechanism found in literature. While we have shown that tempering experiments lead to a simultaneous variation in grain boundaries and surface, and thus may be less significant, experiments such as the microcontact measurements reported in Ref. 7 are difficult if not impossible to explain within a SBLC framework. As an alternative to the developed surface-dominated picture, a combination of contributions of planar defects (causing the second relaxation) and contact-generated Schottky diodes (causing the main relaxation) also seems to be consistent with most of our data. While the latter explanation has some problems, as mentioned at the end of Sec. III, we have to clearly state that from the current experimental basis, it is not possible to definitely conclude which one of the above developed scenarios is correct. However, irrespective of any model description, the bare experimental fact that both relaxations in CCTO vary when the surface of the sample is modified, be it by contact variation or by polishing, shows that surface-related effects play at least some role for the dielectric properties of CCTO. In any case, we do not claim the complete absence of any grain boundary contributions in our or other ceramic samples. Even within our surface-dominated picture, these contributions could arise outside or at the edge of the frequency/temperature window or be superimposed by the surface contributions.

Finally, we want to point out that concerning its intrinsic properties, CCTO is unusual mainly in one way, namely, its rather high  $\epsilon'$  of about 85, arising from a high ionic polarizability.<sup>22</sup> The colossal  $\epsilon'$  of this material is directly related to this high value as it can be assumed that the dielectric constant of the insulating layers (e.g., planar defect or surface depletion layer) is related to that of the bulk, and mainly, the number of charge carriers is different. This high intrinsic  $\epsilon'$ , together with the small thickness of these layers (whatever their origin may be), leads to the apparently colossal  $\epsilon'$ . Concerning possible applications of CCTO in modern microelectronics, one faces two major problems: One, the dielectric loss of CCTO is too high. In addition, as we found for SCs (Fig. 3) and PCs,<sup>9</sup> the values of  $\epsilon'$  at frequencies beyond megahertz, which is a technically highly relevant regime, are far from being colossal. Within the equivalent circuit framework, in order to shift the main relaxation toward higher frequencies, the bulk resistance should be lowered. Thus, if looking for possible alternative materials, one

should aim at lower bulk resistivity and a high or higher intrinsic  $\epsilon'$  as CCTO. To ensure a low overall loss, the resistance of the highly resistive thin layers should be as high as possible. Thus, it is essential to identify the mechanisms leading to these layers. We believe that the presented results may provide at least some hints that will help in solving this question.

## ACKNOWLEDGMENTS

This work was supported by the Commission of the European Communities, STREP: NUOTO, Grant No. NMP3-CT-2006-032644, and by the DFG via the SFB 484. We thank the Anwenderzentrum Material- und Umweltforschung Augsburg for technical support in the ESEM measurements.

- <sup>1</sup>M. A. Subramanian, D. Li, N. Duan, B. A. Reisner, and A. W. Sleight, *J. Solid State Chem.* **151**, 323 (2000).
- <sup>2</sup>A. P. Ramirez, M. A. Subramanian, M. Gardel, G. Blumberg, D. Li, T. Vogt, and S. M. Shapiro, *Solid State Commun.* **115**, 217 (2000).
- <sup>3</sup>C. C. Homes, T. Vogt, S. M. Shapiro, S. Wakimoto, and A. P. Ramirez, *Science* **293**, 673 (2001).
- <sup>4</sup>D. C. Sinclair, T. B. Adams, F. D. Morrison, and A. R. West, *Appl. Phys. Lett.* **80**, 2153 (2002).
- <sup>5</sup>M. A. Subramanian and A. W. Sleight, *Solid State Sci.* **4**, 347 (2002); L. He, J. B. Neaton, M. H. Cohen, D. Vanderbilt, and C. C. Homes, *Phys. Rev. B* **65**, 214112 (2002).
- <sup>6</sup>M. H. Cohen, J. B. Neaton, L. He, and D. Vanderbilt, *J. Appl. Phys.* **94**, 3299 (2003).
- <sup>7</sup>S.-Y. Chung, I.-D. Kim, and S.-J. L. Kang, *Nat. Mater.* **3**, 774 (2004).
- <sup>8</sup>P. Lunkenheimer, V. Bobnar, A. V. Pronin, A. I. Ritus, A. A. Volkov, and A. Loidl, *Phys. Rev. B* **66**, 052105 (2002).
- <sup>9</sup>P. Lunkenheimer, R. Fichtl, S. G. Ebbinghaus, and A. Loidl, *Phys. Rev. B* **70**, 172102 (2004).
- <sup>10</sup>A. P. Ramirez, G. Lawes, V. Butko, M. A. Subramanian, and C. M. Varma, e-print arXiv:cond-mat/0209498.
- <sup>11</sup>T. B. Adams, D. C. Sinclair, and A. R. West, *Adv. Mater. (Weinheim, Ger.)* **14**, 1321 (2002); B. A. Bender and M.-J. Pan, *Mater. Sci. Eng., B* **117**, 339 (2005).
- <sup>12</sup>P. Lunkenheimer, M. Resch, A. Loidl, and Y. Hidaka, *Phys. Rev. Lett.* **69**, 498 (1992); A. I. Ritus, A. V. Pronin, A. A. Volkov, P. Lunkenheimer, A. Loidl, A. S. Shcheulin, and A. I. Ryskin, *Phys. Rev. B* **65**, 165209 (2002); V. Bobnar, P. Lunkenheimer, J. Hemberger, A. Loidl, F. Lichtenberg, and J. Mannhart, *ibid.* **68**, 155115 (2002); P. Lunkenheimer, T. Rudolf, J. Hemberger, A. Pimenov, S. Tachos, F. Lichtenberg, and A. Loidl, *ibid.* **68**, 245108 (2003).
- <sup>13</sup>B. Renner, P. Lunkenheimer, M. Schetter, A. Loidl, A. Reller, and S. G. Ebbinghaus, *J. Appl. Phys.* **96**, 4400 (2004); P. Lunkenheimer, T. Götzfried, R. Fichtl, S. Weber, T. Rudolf, A. Loidl, A. Reller, and S. G. Ebbinghaus, *J. Solid State Chem.* **179**, 3965 (2006).
- <sup>14</sup>S. Krohns, P. Lunkenheimer, S. G. Ebbinghaus, and A. Loidl, *Appl. Phys. Lett.* **91**, 022910 (2007); **91**, 149902 (2007).
- <sup>15</sup>J. L. Zhang, P. Zheng, C. L. Wang, M. L. Zhao, J. C. Li, and J. F. Wang, *Appl. Phys. Lett.* **87**, 142901 (2005).
- <sup>16</sup>G. Zang, J. Zhang, P. Zheng, J. Wang, and C. Wang, *J. Phys. D* **38**, 1824 (2005); B. Shri Prakash and K. B. R. Varma, *Physica B (Amsterdam)* **382**, 312 (2006); L. Ni, X. M. Chen, X. Q. Liu, and R. Z. Hou, *Solid State Commun.* **139**, 45 (2006).
- <sup>17</sup>N. Kolev, R. P. Bontchev, A. J. Jacobson, V. N. Popov, V. G. Hadjiev, A. P. Litvinchuk, and M. N. Iliev, *Phys. Rev. B* **66**, 132102 (2002); *ibid.* **71**, 014118 (2005); J. Li, A. W. Sleight, and M. A. Subramanian, *Solid State Commun.* **135**, 260 (2005); M.-H. Whangbo and M. A. Subramanian, *Chem. Mater.* **18**, 3257 (2006).
- <sup>18</sup>L. Fang, M. Shen, and W. Cao, *J. Appl. Phys.* **95**, 6483 (2004).
- <sup>19</sup>C. C. Wang and L. W. Zhang, *Appl. Phys. Lett.* **88**, 042906 (2006).
- <sup>20</sup>R. Böhmer, M. Maglione, P. Lunkenheimer, and A. Loidl, *J. Appl. Phys.* **65**, 901 (1989); U. Schneider, P. Lunkenheimer, A. Pimenov, and R. Brand, *Ferroelectrics* **249**, 89 (2001).
- <sup>21</sup>S. R. Elliott, *Adv. Phys.* **36**, 135 (1987); *ibid.* **31**, 553 (1982).
- <sup>22</sup>Ch. Kant, T. Rudolf, F. Mayr, S. Krohns, P. Lunkenheimer, S. G. Ebbinghaus, and A. Loidl, *Phys. Rev. B* **77**, 045131 (2008).
- <sup>23</sup>N. F. Mott and E. A. Davis, *Electronic Processes in Non-Crystalline Materials* (Clarendon, Oxford, 1979).
- <sup>24</sup>L. Zhang and Z.-J. Tang, *Phys. Rev. B* **70**, 174306 (2004).
- <sup>25</sup>J. H. Hwang, K. S. Kirkpatrick, T. O. Mason, and E. J. Garboczi, *Solid State Ionics* **98**, 93 (1997).
- <sup>26</sup>D. Starešinić, P. Lunkenheimer, J. Hemberger, K. Biljaković, and A. Loidl, *Phys. Rev. Lett.* **96**, 046402 (2006).
- <sup>27</sup>D. Starešinić, K. Biljaković, W. Brütting, K. Hossein, P. Monceau, H. Berger, and F. Levy, *Phys. Rev. B* **65**, 165109 (2002).
- <sup>28</sup>D. Starešinić (private communication).
- <sup>29</sup>A. Tselev, C. M. Brooks, S. M. Anlage, H. Zheng, L. Salamanca-Riba, R. Ramesh, and M. A. Subramanian, *Phys. Rev. B* **70**, 144101 (2004).
- <sup>30</sup>S. Ke, H. Huang, and H. Fan, *Appl. Phys. Lett.* **89**, 182904 (2006).
- <sup>31</sup>A similar experiment was performed in Ref. 19; however, a complete vanishing of the second relaxation was claimed only after reducing the sample thickness by 0.82 mm, which would imply a too thick layer to arrive at colossal values of  $\epsilon'$ . Possibly, reoxidation occurred during polishing in air.
- <sup>32</sup>These considerations are valid for SCs and PCs; in the latter case, a diode forms at each outer surface of the grains facing the electrode material. These diodes, which are connected in parallel, act as a single diode.
- <sup>33</sup>G. Deng, T. Yamada, and P. Muralt, *Appl. Phys. Lett.* **91**, 202903 (2007).
- <sup>34</sup>Y. Zhu, J. C. Zheng, L. Wu, A. I. Frenkel, J. Hanson, P. Northrup, and W. Ku, *Phys. Rev. Lett.* **99**, 037602 (2007).